*Progress In Electromagnetics Research C, Vol. 122, 199–213, 2022*

# Tracking Model of Joint Electromagnetic Signals of Naval Targets Based on Small-Scale Platform

**Qi Liu, Zhaolong Sun, Runxiang Jiang*, Jiawei Zhang, and Kui Zhu**

**Abstract**—For the tracking problem of moving targets by small-scale platforms, this paper firstly proposed a ship target tracking model with joint electromagnetic signals based on point charge theory and point magnetic charge theory. Then, the target tracking was simulated and verified with the progressive update extended Kalman filter algorithm as the filtering unit and the small-scale platform as the sensor-carrying platform. Finally, the laboratory model validation was carried out, and the simulated source experiment and ship model experiment were conducted, respectively. The simulation results show that the tracking method with the joint electromagnetic signal can achieve a tracking error less than 5 m in the range of 6 times the ship length. The results of the model experiments further verify the simulation results. When the signal-to-noise ratio is only 5, it can also achieve at least 2 times the ship's length of tracking, which can effectively solve the problem of poor tracking caused by the small size of the sensor carrying platform and the small number of sensors.

## 1. INTRODUCTION

Underwater electromagnetic field is one of the important physical field characteristics of ships. With the continuous development of electromagnetic stealth technology of ships, how to achieve long-range tracking of ship targets after detecting electromagnetic signals is especially critical.

The current research is mainly focused on tracking a single electric field or a single magnetic field signal. In terms of electric field tracking, the main research focuses on tracking the electric field modulus, slope, gradient, etc. [1]. Luo et al. achieved target tracking by measuring the gradient value of the electric field in the vertical direction [2]. Wu [3] and Zhao [4] proved that the electric dipole position can be successfully solved by using the analytical inversion method through model derivation. Bao et al. [5] obtained the electric dipole source by arranging two three-axis electric field sensors in the vertical direction. Wang [6] used a hybrid electric dipole method to locate different values of the vertical component as well as the horizontal component of the electric field. The above-mentioned analytical method to achieve target tracking has the shortage of large computational volume, so the Kalman filter algorithm is more widely used in filtering methods to track the electric field target. Yu et al. [7] successfully applied the extended Kalman filter algorithm to electrostatic field tracking of ships. Donati and Le Cadre [8] used the underwater electric field information and achieved the estimation of target position and heading angle and other states based on GLRT and Monte Carlo criterion. Zhang et al. [9] proposed a target tracking algorithm based on static potential difference, which can achieve target tracking with fewer sensors.

In the field of magnetic field tracking, the United States has used the magnetic field gradiometer array to achieve the location tracking of magnetic dipole sources as early as 1975 [10] and achieved the unique determination of magnetic dipole source parameters in combination with the magnetic field tensor when the three components of the magnetic field were known in the 1990s [11]. Wahlström et al. [12] and Birsan [13] successfully achieved the tracking of ship magnetic signals. Wilson et al. [14] and Emerson et al. [15] achieved the tracking of magnetic sources and the calculation of parameters

*Received 2 June 2022, Accepted 20 July 2022, Scheduled 12 August 2022*
* Corresponding author: Runxiang Jiang (jiang_runxiang@163.com).
The authors are with the Naval University of Engineering, Wuhan 430000, China.

through the eigenvalues and eigenvectors of the magnetic tensor, combined with the sphere model. In China, there are more achievements in tracking research for ship magnetic signals from Naval University of Engineering and Shanghai Jiao Tong University: a team led by Prof. Gong from Naval University of Engineering studied tracking methods for moving and stationary ship targets [16, 17], which can achieve tracking of magnetic source targets. Wu and Sun [18] proposed a recursive update Kalman filter-based magnetic dipole target tracking, which can overcome large initial errors. Shan et al. [19] proposed a new Kalman filter and verified that it can track magnetic dipoles by simulation.

In electromagnetic joint tracking, mostly seen in medical, communication, and industrial applications [20–22], there is less research in the joint tracking of electromagnetic signals for naval targets and also less research in the tracking of targets based on small-scale platforms carrying sensors. There are disadvantages of small spacing and small number of sensor placements due to the limitations of the scale of the small-scale platforms themselves, and at the same time, the target signals collected between sensors are not highly differentiated from each other, resulting in less target information, so it is more difficult to achieve effective tracking.

In order to solve the target tracking problem of small-scale platform, this paper firstly establishes the target tracking model of joint electromagnetic signal, adopts point electric charge and point magnetic charge together to simulate the target source field distribution, deploys two potential sensors and one triaxial fluxgate sensor with the structure of underwater weapon platform as the piggyback platform, and uses the potential difference and the three components of magnetic field as the tracking signal. Then, an asymptotic update extended Kalman filter is used as the filtering unit to simulate and verify the joint tracking model. Finally, the equivalent source experiment and ship model experiment are carried out sequentially in the laboratory to verify the model.

## 2. DERIVATION OF TRACKING MODEL FOR JOINT ELECTROMAGNETIC SIGNAL

### 2.1. Tracking Principle of Electric and Magnetic Signals

The modeling method of point charge is used to calculate the ship's electrical signal. Assuming that there are $N$ point charges in seawater, let the coordinates of the point charge $S_i$ be $(x_i, y_i, z_i)$, $i = 1, 2, \ldots, N$. The ship contains $M$ sensor measurement points (field points) around the ship, and the coordinates of the measurement points are $(x_j, y_j, z_j)$, $j = 1, 2, \ldots, M$. Let the charge of point charge $S_i$ be $Q_U = [Q_{U1}, Q_{U2}, \ldots, Q_{UN}]$, and the value of the potential at measurement point $P_j$ be the linear superposition of the potential generated by the $i$th point charge $S_i$ at $P_j$. The potential at measurement point $P_j$ is calculated as:

$$U_j = \frac{1}{4\pi\sigma} \sum_{i=1}^{N} Q_{Ui} K(S_i, P_j) \tag{1}$$

where $K(S_i, P_j)$ is the distance function between the point charge $S_i$ measurement points $P_j$ in the three-layer medium space of air-seawater-seabed, and the expressions are:

$$\begin{aligned} K(S_i, P_j) \;=\; & \frac{1}{\sqrt{(x_j - x_i)^2 + (y_j - y_i)^2 + (z_j - z_i)^2}} \\ & + \frac{1}{\sqrt{(x_j - x_i)^2 + (y_j - y_i)^2 + (z_j + z_i - 2h)^2}} \\ & + \sum_{m=1}^{\infty} k^m \left[ \begin{array}{l} \dfrac{1}{\sqrt{(x_j - x_i)^2 + (y_j - y_i)^2 + (z_j + z_i - 2h + 2mH)^2}} \\ + \dfrac{1}{\sqrt{(x_j - x_i)^2 + (y_j - y_i)^2 + (z_j + z_i - 2h - 2mH)^2}} \\ + \dfrac{1}{\sqrt{(x_j - x_i)^2 + (y_j - y_i)^2 + (z_j - z_i + 2mH)^2}} \\ + \dfrac{1}{\sqrt{(x_j - x_i)^2 + (y_j - y_i)^2 + (z_j - z_i - 2mH)^2}} \end{array} \right] \end{aligned} \tag{2}$$

where $h$ is the depth of deployment of the sensor, $H$ the depth of seawater, $\sigma_2$ the conductivity of seawater, $\sigma_3$ the conductivity of the seabed, $k = (\sigma_3 - \sigma_2)/(\sigma_3 + \sigma_2)$ the reflection coefficient of the seabed, and $m$ the number of reflective layers, whose upper limit can be taken as $10 \sim 20$ in practical calculations.

Therefore, when the potential at the measurement point is known, the position of the measurement point relative to the point charge can also be derived from the inversion of Equation (1), thus enabling the tracking and positioning of the electrical signal.

For magnetic signals, from [23], it is assumed that there exists a point magnetic charge in space with a magnetic charge of $Q_B$, and the magnetic induction generated in space by the magnetic charge at this point is

$$\mathbf{B} = \frac{\mu_0}{4\pi}\frac{Q_B}{r^3}\mathbf{r} \tag{3}$$

where $\mu_0$ is the vacuum permeability; the vector $\mathbf{r}$ points from the point charge $P$ to the field point $S$; $r$ is the distance between the point charge and the field point.

Similarly, let the magnetic charge of the point magnetic charge $S_i$ be $\mathbf{Q}_B = [Q_{B1}, Q_{B2}, \ldots, Q_{BN}]$. The magnetic induction $P_j$ generated at the measurement point $B_j = [B_{xj}, B_{yj}, B_{zj}]$ can be calculated according to the following equation.

$$\begin{cases} B_{xj} = \sum_{i=1}^{N} Q_{Bi} A_x(S_i, P_j) \\ B_{yj} = \sum_{i=1}^{N} Q_{Bi} A_y(S_i, P_j) \\ B_{zj} = \sum_{i=1}^{N} Q_{Bi} A_z(S_i, P_j) \end{cases} \tag{4}$$

$$\begin{cases} A_x(S_i, P_j) = \frac{\mu_0}{4\pi}\frac{x_j - x_i}{r^3} \\ A_y(S_i, P_j) = \frac{\mu_0}{4\pi}\frac{y_j - y_i}{r^3} \\ A_z(S_i, P_j) = \frac{\mu_0}{4\pi}\frac{z_j - z_i}{r^3} \end{cases} \tag{5}$$

where $A_x(S_i, P_j)_y(S_i, P_j)_z(S_i, P_j)$ is the distance between each point charge and each field point, and $Q_{Bi}$ is the magnetic charge of the first point charge, $r = \sqrt{(x_j - x_i)^2 + (y_j - y_i)^2 + (z_j - z_i)^2}$.

Therefore, the magnetic induction intensity at the measurement point is known, and the position of the measurement point relative to the magnetic charge can be inferred from Equation (4) and Equation (5), thus enabling the tracking and positioning of the magnetic signal.

### 2.2. State Space Tracking Model for the Joint Electromagnetic Signal of a Ship

In actual ship target tracking, when the ship's electric/magnetic cloaking device is on, the intensity of the ship's electromagnetic signal will be reduced. The essence of target tracking is the inversion of the model, and using the joint signal method can effectively improve the diversity of the model, so that the diversity of source information can be increased, thus improving the tracking effect.

Based on the state space tracking model of a single signal, this section develops a joint tracking state model of the ship's electromagnetic signal: $N_1$ point charges, $N_2$ point magnetic charges, 2 Ag/AgCl sensors and 1 triaxial fluxgate sensor are used to model the ship's electromagnetic field state.

The positions of 2 Ag/AgCl sensors are $P_1$ and $P_2$, respectively; the position of 1 triaxial fluxgate sensor is $P_3$; the random disturbance during the ship's motion is $\mathbf{w}_k$; and the sampling interval is $T$.

Then the state transition equation of the ship's target from the moment $k-1$ to the moment $k$ can be:

$$\begin{cases} x_k = x_{k-1} + v_{x,k-1}T + \frac{1}{2}w_{x,k-1}T^2 \\ y_k = y_{k-1} + v_{y,k-1}T + \frac{1}{2}w_{y,k-1}T^2 \\ v_{x,k} = v_{x,k-1} + w_{x,k-1}T \\ v_{y,k} = v_{y,k-1} + w_{y,k-1}T \\ \mathbf{Q}_{U,k} = \mathbf{Q}_{U,k-1} + \mathbf{w}^Q_{U,k-1}T \\ \mathbf{Q}_{B,k} = \mathbf{Q}_{B,k-1} + \mathbf{w}^Q_{B,k-1}T \end{cases} \tag{6}$$

The coefficient matrices $\mathbf{\Phi}$ and $\mathbf{\Psi}$ in this tracking model are:

$$\mathbf{\Phi} = \begin{bmatrix} \mathbf{I}_{2\times2} & T\mathbf{I}_{2\times2} & \mathbf{0}_{2\times(N_1+N_2)} \\ \mathbf{0}_{(2+N_1+N_2)\times2} & \mathbf{I}_{(2+N_1+N_2)\times(2+N_1+N_2)} \end{bmatrix} \tag{7}$$

$$\mathbf{\Psi} = \begin{bmatrix} \frac{T^2}{2}\mathbf{I}_{2\times2} & \mathbf{0}_{2\times(N_1+N_2)} \\ T\mathbf{I}_{(2+N_1+N_2)\times(2+N_1+N_2))} \end{bmatrix} \tag{8}$$

The state vector $\mathbf{x}_k$ is:

$$\mathbf{x}_{k-1} = [x_{k-1},\ y_{k-1},\ v_{x,k-1},\ v_{y,k-1},\ \mathbf{Q}_{U,k-1},\ \mathbf{Q}_{B,k-1}]^T \tag{9}$$

The noise vector is:

$$\mathbf{w}_k = [w_{x,k},\ w_{y,k},\ \mathbf{w}_{U,k},\ \mathbf{w}_{B,k}]^T \tag{10}$$

The observed quantity of electric signal is the potential difference, and the observed quantity of magnetic signal is the three components of magnetic field, then the observation equation of ship's magnetic signal can be obtained as:

$$\mathbf{y}_k = \mathbf{h}(\mathbf{x}_k) + \mathbf{u}_k = \begin{bmatrix} \frac{1}{4\pi\sigma_2}\left[\sum_{i=1}^{N_1} Q_{Ui}K(S_i,P_1) - \sum_{i=1}^{N_1} Q_{Ui}K(S_i,P_2)\right] \\ \sum_{i=1}^{N} Q_{Bi}A_x(S_i,P_3) \\ \sum_{i=1}^{N} Q_{Bi}A_y(S_i,P_3) \\ \sum_{i=1}^{N} Q_{Bi}A_z(S_i,P_3) \end{bmatrix} + \begin{bmatrix} u_1 \\ u_2 \\ u_3 \\ u_4 \end{bmatrix} \tag{11}$$

The state space model of the joint EM signal tracking problem of a ship can be obtained from Equations (6)–(11).

### 2.3. Progressive Update Extended Kalman Filtering Algorithm

For the nonlinear process of ship motion, the Kalman filter can be used to track the target, and according to the existing research, the progressive update extended Kalman filter (PUEKF) can achieve better results on the ship electric field target tracking [24–26]. The specific algorithm steps are as follows:

1, Time update process:

$$\begin{cases} \mathbf{P}_{k|k-1} = \mathbf{\Phi}\mathbf{P}_{k-1|k-1}\mathbf{\Phi}^T + \mathbf{R}_{w,k-1} \\ \widehat{\mathbf{x}}_{k|k-1} = \mathbf{\Phi}\widehat{\mathbf{x}}k|k-1 \end{cases} \tag{12}$$

where $\mathbf{P}_{k|k-1}$ is the prediction error covariance matrix; $\widehat{\mathbf{x}}_{k|k-1}$ is the linearized expansion point.

2, Observation update process:

(1) Initialize the prediction error covariance matrix $\mathbf{P}$ and linearize the expansion point $\widehat{\mathbf{x}}$:

$$\begin{cases} \mathbf{P}_{0|a=1} = \mathbf{P}_{k|k-1} \\ \widehat{\mathbf{x}}_{0|a=1} = \widehat{\mathbf{x}}_{k|k-1} \end{cases} \tag{13}$$

(2) Make $a = 1, 2, \ldots, A$, a loop to observe the update process:

$$\begin{cases} \mathbf{S}_{a-1} = \mathbf{H}_{a-1}\mathbf{P}_{a-1}\mathbf{H}_{a-1}^T + \mathbf{R}_{u,k-1}/\lambda \\ \mathbf{K}_a = \mathbf{P}_{a-1}\mathbf{H}_{a-1}^T\mathbf{S}_{a-1}^{-1} \\ \widehat{\mathbf{x}}_a = \widehat{\mathbf{x}}_{a-1} + \mathbf{K}_a(\mathbf{y}_k - \mathbf{h}(\widehat{\mathbf{x}}_{a-1})) \\ \mathbf{P}_a = (\mathbf{I} - \mathbf{K}_a\mathbf{H}_{a-1})\mathbf{P}_{a-1} \end{cases} \tag{14}$$

where $A$ is the total number of executions of the cycle; $\mathbf{S}$ is the process variable; the parameter $\lambda = 1/A$, $\mathbf{K}$ is the Kalman gain; $\mathbf{H}_{a-1} = \frac{\partial h(x_{a-1})}{\partial x_{a-1}}$ is the first-order partial derivative matrix of $\mathbf{h}(\mathbf{x}_{a-1})$ at $\widehat{\mathbf{x}}_{a-1}$; and $\mathbf{h}(\mathbf{x}_{a-1})$ is the observed quantity obtained by solving A based on the observation equation.

(3) Update the state quantities $\mathbf{P}_{k|k}$ and $\widehat{\mathbf{x}}_{k|k}$.

According to the given initial conditions $\widehat{\mathbf{x}}_0$ and $\mathbf{P}_0$, the above time update process and state update process are executed from the moment of $k = 1$. When the update of all moments is completed, the estimated value of the signal to be observed at each time can be obtained, and the position tracking of the target is completed.

## 3. SIMULATION VERIFICATION OF TARGET TRACKING BASED ON SMALL-SCALE PLATFORM

### 3.1. Simulation Parameter Setting

In this paper, the tracking effect of different tracking models at different depths is simulated and analyzed by taking an underwater weapon platform as an example.

In order to judge the tracking effect, the two-parametric numbers of $x$, $y$, and distance at moment $k$ for the real and predicted trajectories are calculated separately as a measure of tracking effect:

$$\begin{cases} AE_{k,x} = \|x\|_2 = \sqrt{(x_{k,estimate} - x_{k,real})^2} \\ AE_{k,y} = \|y\|_2 = \sqrt{(y_{k,estimate} - y_{k,real})^2} \\ AE_{k,d} = \|d\|_2 = \sqrt{(x_{k,estimate} - x_{k,real})^2 + (y_{k,estimate} - y_{k,real})^2} \end{cases} \tag{15}$$

where $x_{k,estimate}$ is the estimated value of the $x$ direction at the $k$th moment; $y_{k,estimate}$ is the estimated value of the $y$ direction at the $k$th moment; $x_{k,real}$ is the true value of the $x$ direction at the $k$th moment; $y_{k,real}$ is the true value of the $y$ direction at the $k$th moment.

Here it is specified that the tracking is considered effective when $AE_{k,d} \leq 5\,\text{m}$, i.e., the distance error is not greater than 5 m.

In order to effectively evaluate the tracking effect and exclude the influence caused by the change of target movement speed, the effective tracking distance $S_{effect}$ at a distance error of not more than 5 m is used to evaluate the tracking effect. $a$ is the tracking scale factor, and $L$ is the ship's length of the ship. The calculation method is as follows:

$$S_{effect} = a \cdot L \tag{16}$$

In order to investigate the tracking effect at different depths, the sensors were placed in the sea at different depths to compare the tracking effects. The sensors were placed at depths of 20 m, 30 m, 40 m, 50 m, 60 m, 70 m, 80 m, 90 m, and 100 m, and the basic simulation parameters were set as shown in Table 1.

In the actual target tracking, the ship's length $L$, ship's width $b$, and draft depth $a$ are all parameters to be determined. The spatial distribution of point charge and point magnetic charge is determined by the ship's length $L$ and ship's width $b$, and the ship's length $L$ is generated randomly in the range [80 m, 160 m]. In order to construct the spatial distribution of point charge and point magnetic charge,

**Table 1.** Basic simulation parameter setting table.

| Parameter name | Parameter setting |
|---|---|
| Seawater depth (m) | 100 |
| Seawater conductivity (S/m) | 4 |
| Sea bed conductivity (S/m) | 0.04 |
| Sampling frequency (Hz) | 20 |
| Total simulation time (s) | 120 |
| Ship length (m) | $L$ |
| Vessel width (m) | $b$ |
| Draught depth (m) | $a$ |

the relationship between the ship's length $L$ and the ship's width $b$ and draught depth $a$ is assumed to be $b = L/10$ and $a = L/20$.

The target is equated to a uniform ellipsoidal model, and it is known from [27] that when the measurement depth is greater than 0.2 times the ship's length, at least 3 point charge model electrical sources can be used. Therefore, assuming an average ship's length of 100 m, when the distance between the sensor and the target is not less than 20 m, 3 point charge simulated electrical sources can be used; it is known from [28] that two point magnetic charges can be equated to 1 magnetic dipole source in 1 direction, and 6 point magnetic charges can be used to simulate the magnetic source. The spatial distribution of point charges and point magnetic charges in the ellipsoid is shown in Figure 1.

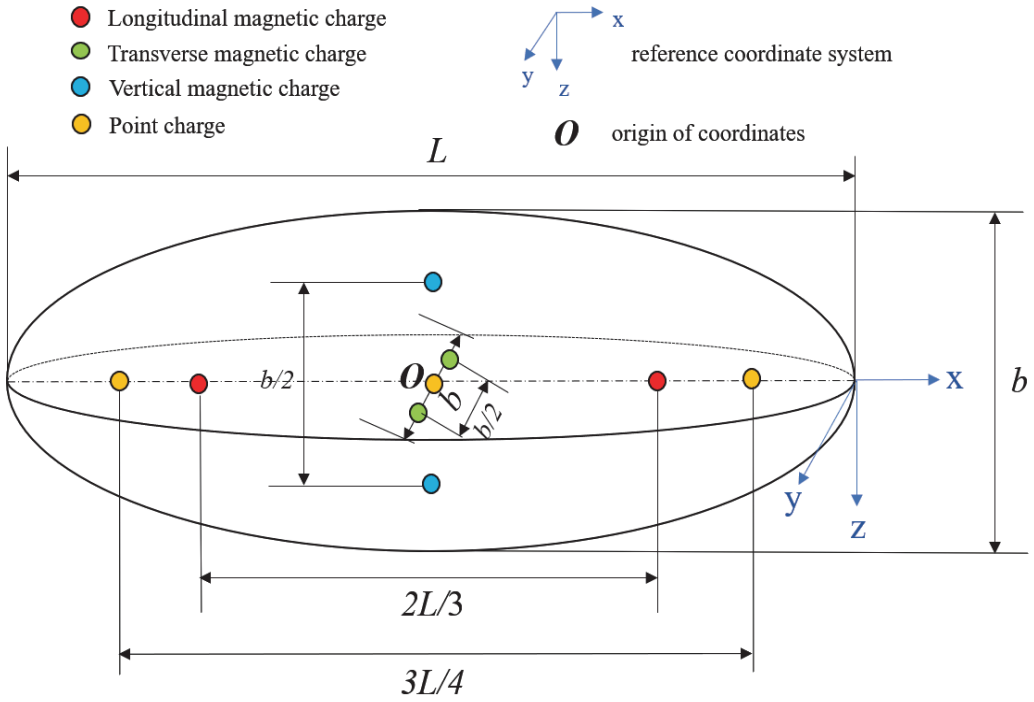


**Figure 1.** Spatial distribution of point charges and point magnetic charges in the ellipsoid.

### 3.2. Target Tracking Simulation Validation with Joint Electromagnetic Signals

Combined with the structural dimensions of the underwater weapon platform, this section uses two Ag/AgCl sensors and one three-axis fluxgate sensor to build a tracking system suitable for the underwater weapon platform, and the sensor installation schematic is shown in Figure 2.

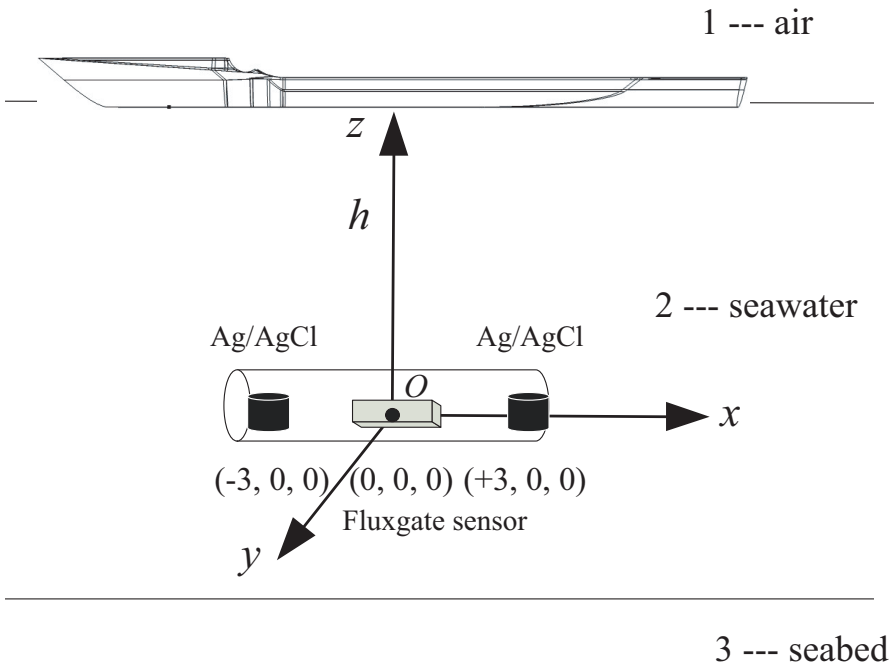


**Figure 2.** Schematic diagram of the sensor installation on the in-water weapon platform.

The recursive extended Kalman filter parameters are set as in Table 2. Random fluctuating disturbances obeying Gaussian distribution with peak-to-peak values of 2.4 μT and 0.8 nT are added to the potential and magnetic field signals, respectively, according to the perturbation characteristics of the electric and magnetic field signals in the real ocean [29, 30].

The tracking results are shown in Figure 3 when the measured depth is 20 m.

The tracking results for different depths are shown in Table 3.

The simulation results show that

(1) The method of joint tracking of electromagnetic signals by deploying two Ag/AgCl sensors and one fluxgate sensor on a small-scale platform with an underwater weapon as an example is effective.

(2) The effective tracking distance of the simulation can achieve the tracking error less than 5 m within 6.1 times in the case of natural interference.

(3) The effective tracking distance gradually decreases with the increase of the measurement depth, which is caused by the signal strength gradually decreasing as the sensor becomes farther away from the target source.

## 4. JOINT ELECTROMAGNETIC SIGNAL TRACKING EXPERIMENT WITH SIMULATED SOURCE MODEL

In order to verify the tracking effect of the model, the simulation source is first used to validate the model approach. The top view of the experimental arrangement is shown in Figure 4.

The actual length of the target is assumed to be 100 m, and the scaling ratio is 1 : 100. 1 m long simulated source is used as the target source in this section. The magnetic signal comes from the magnetic field of the analog source itself, and the electric signal comes from the positive and negative electrodes with constant current applied to the two ends of the analog source at intervals. The distance between the electrodes is 60 cm, and the overall layout of the test is shown in Figure 5. The coordinate

**Table 2.** Parameter settings in recursive extended Kalman filter.

| Parameter name | Parameter setting | |
|---|---|---|
| Target ideal starting coordinates | $(400\,\text{m}, -400\,\text{m})$ | |
| Target actual starting coordinates | $(350\,\text{m}, -400\,\text{m})$ | |
| Target ideal velocity | $(-10\,\text{m/s}, 13\,\text{m/s})$ | |
| Actual velocity of target | $(-11\,\text{m/s}, 12\,\text{m/s})$ | |
| Initial value of coordinates of point charge | $Q_{U1}(-\frac{3L}{8}, 0, a)$ | |
| | $Q_{U2}(0, 0, a)$ | |
| | $Q_{U3}(\frac{3L}{8}, 0, a)$ | |
| Initial value of coordinates of point magnetic charge | Longitudinal | $Q_{B1}(-\frac{L}{3}, 0, a)$ |
| | | $Q_{B2}(\frac{L}{3}, 0, a)$ |
| | Horizontal | $Q_{B3}(0, \frac{b}{4}, a)$ |
| | | $Q_{B4}(0, -\frac{b}{4}, a)$ |
| | Vertical | $Q_{B5}(0, 0, a + \frac{b}{4})$ |
| | | $Q_{B6}(0, 0, a - \frac{b}{4})$ |
| Initial value of electric charge | $[-35\ 75\ -40]$ | |
| Initial value of magnetic charge | $[-45\ 10\ -5\ -580\ -35]$ | |
| Potential sensor I coordinates | $(-200,\ 400,\ h)$ | |
| Potential sensor II coordinates | $(-206,\ 400,\ h)$ | |
| Fluxgate sensor coordinates | $(-203,\ 400,\ h)$ | |
| Process noise $x$ and $y$ direction acceleration noise intensity $\eta_x$ and $\eta_y$ | 0.1, 0.1 | |
| Process noise matrix $\mathbf{w}_k$ | $\begin{bmatrix} 0.01\mathbf{I}_{2\times2} & \mathbf{0}_{2\times11} \\ \mathbf{0}_{11\times2} & 10^{-6}\mathbf{I}_{11\times11} \end{bmatrix}$ | |

**Table 3.** Tracking results of different depths.

| **Tracking error not more than 5 m** | | | | | | | | | |
|---|---|---|---|---|---|---|---|---|---|
| Depth (m) | 20 | 30 | 40 | 50 | 60 | 70 | 80 | 90 | 100 |
| $S_{effect}^{UB}$ | $6.1L$ | $6.0L$ | $5.7L$ | $5.1L$ | $5.0L$ | $4.4L$ | $4.1L$ | $3.3L$ | $2.7L$ |

system is established by using the lateral pool edge parallel to the starting motion of the target as the coordinate origin.

In order to verify the applicability of the tracking method, this paper conducts experimental verification of the tracking process for targets with different positive transverse distances at different depths.

The parameters of the scaling test are set according to the simulation parameters, as shown in Table 4.

From Equation (15), it can be seen that when a 1 : 100 scaled-down model is used for verification in the laboratory, the effective tracking distance is considered to be effective when the effective tracking distance is $AE_{k,d} \leq 0.05\,\text{m}$. Due to the space limitation of the laboratory pool, the movable range of the target is about $5.5L$. When the measured water depth is 20 cm, the tracking results of the positive transverse distance of the target are 10 cm, 20 cm, and 40 cm, respectively, are shown in Figure 6.

As can be seen from Figure 6, when the measured water depth is 20 cm, the deviation of the joint tracking distance of electromagnetic signals with different positive horizontal distances is less than 0.05 m, and the effective distance is $5.5L$, which is the whole length of the target that can be moved in the test. The smaller the positive horizontal distance is, the better the tracking effect is, and the

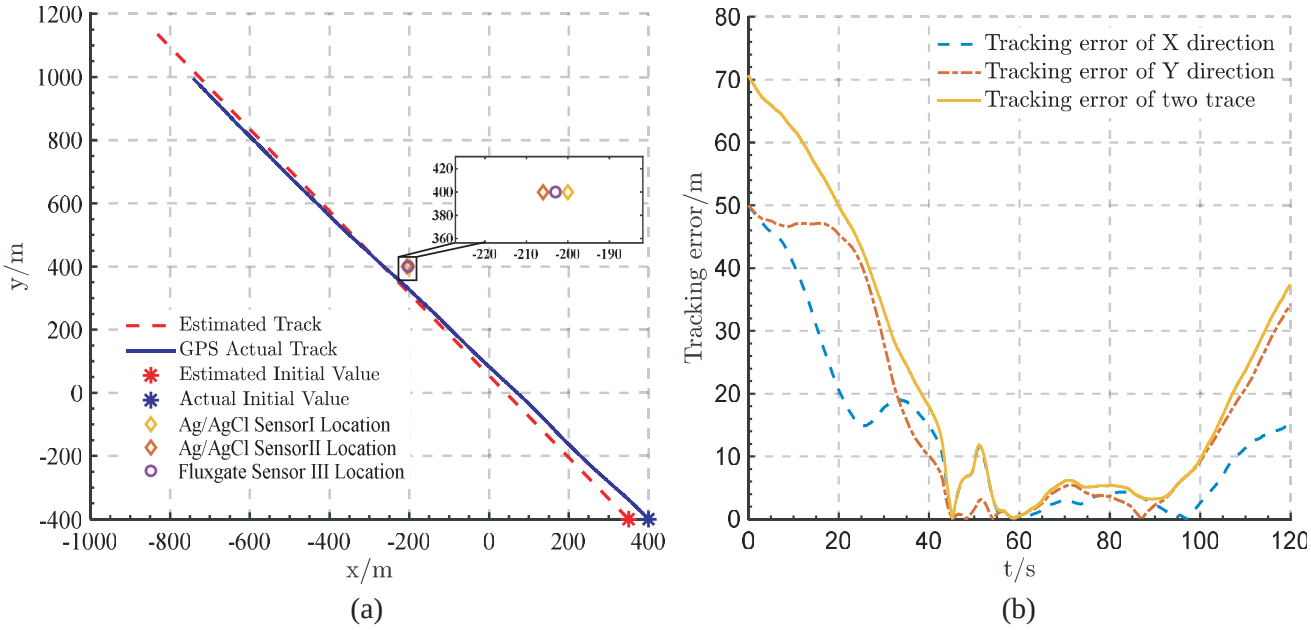


**Figure 3.** When the measured depth is 20 m, the tracking calculation result of electromagnetic signals. (a) The target tracking process diagram. (b) The tracking error result graph.

tracking error increases with the increase of positive horizontal distance.

The tracking results of single signal and joint electromagnetic signal are shown in Table 5.

From the analog source model experiments, it is known that:

(1) The joint electromagnetic signal target tracking method can achieve effective tracking: when the measured water depth is 20 cm, the joint electromagnetic signal tracking method can achieve the error of tracking 5.5 times the ship's length less than 0.05 m when the positive transverse distance is not greater than 40 cm.

(2) The tracking distance decreases with the increase of the positive horizontal distance and the increase of the measuring depth.

**Table 4.** Setting table of iron bar shrinkage test parameters.

| **Parameter name** | | **Parameter setting** |
|---|---|---|
| Pool length | | 8 m |
| Pool width | | 5 m |
| Target starting coordinates I | | (0 m, 1.20 m, 0 m) |
| Target starting coordinates II | | (0 m, 1.30 m, 0 m) |
| Target starting coordinates III | | (0 m, 1.50 m, 0 m) |
| Target movement speed | | (0.07 m/s, 0 m/s, 0 m/s) |
| Single signal tracking | Sensor I Coordinate | (266.8 cm, 110 cm, $h$) |
| | Sensor II coordinates | (271.2 cm, 112 cm, $h$) |
| Electromagnetic signal tracking | Ag/AgCl sensor I coordinates | (266.8 cm, 110 cm, $h$) |
| | Ag/AgCl sensor II coordinate | (271.2 cm, 114 cm, $h$) |
| | Fluxgate sensor III coordinate | (271.2 cm, 112 cm, $h$) |
| Sampling frequency | | 20 Hz |
| Electrode current | | 150 mA |

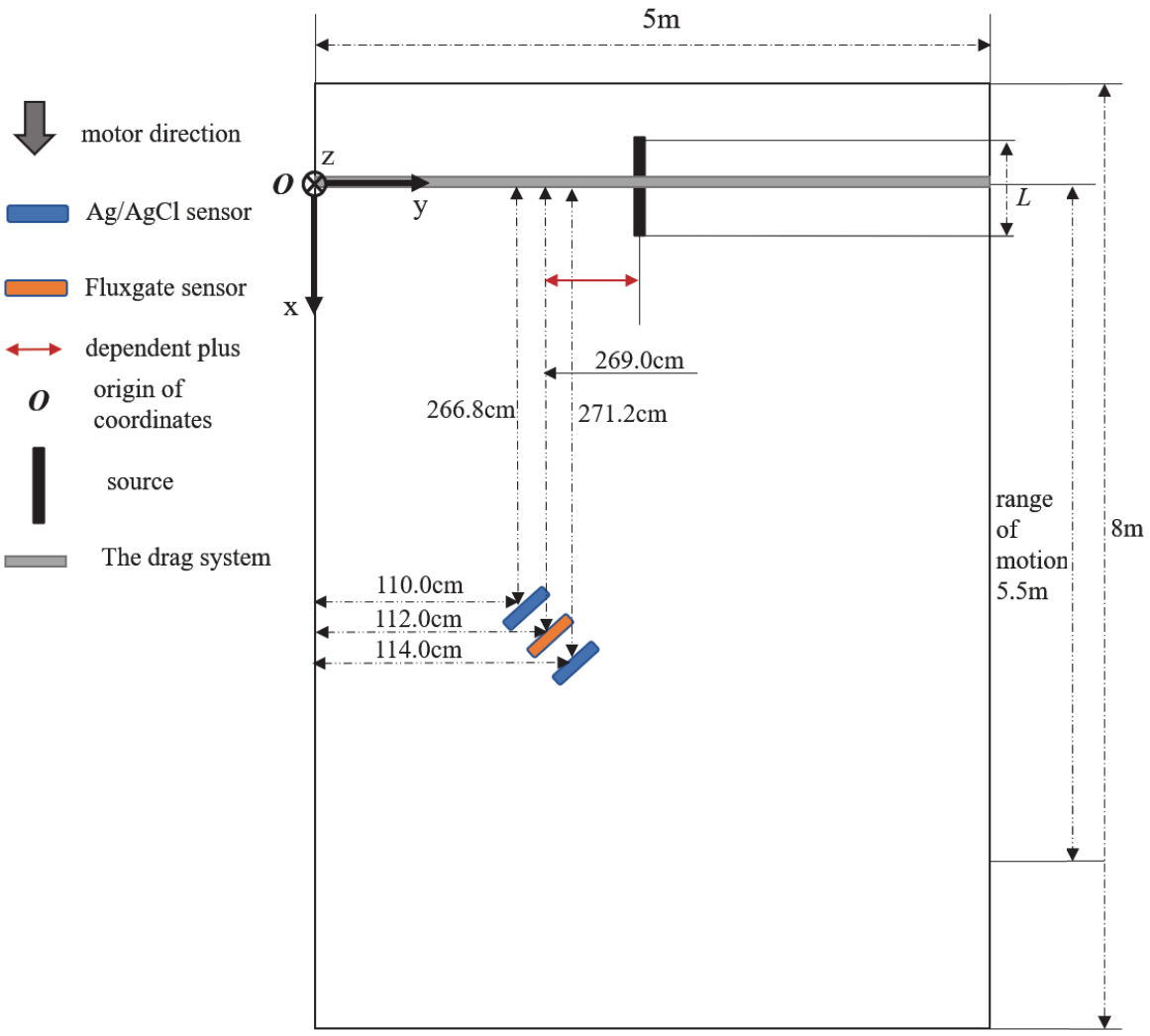


**Figure 4.** Top view of experimental layout.

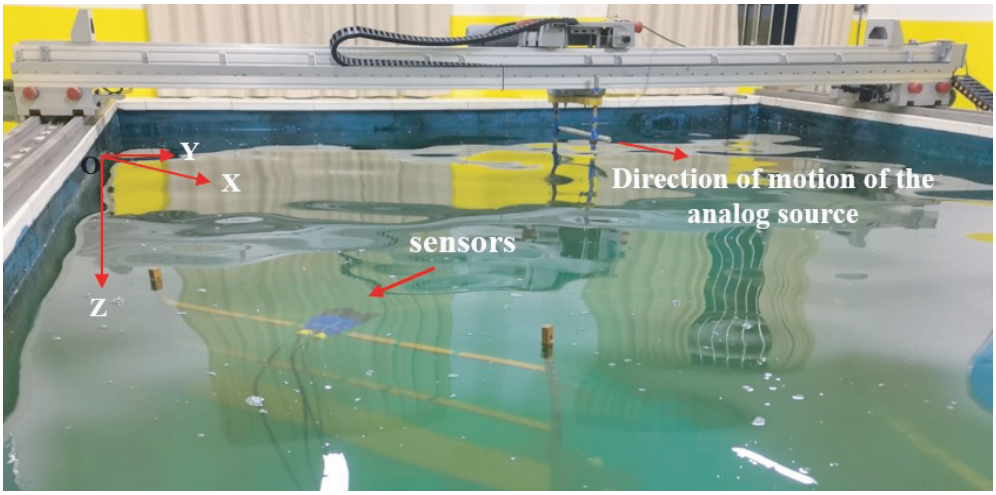


**Figure 5.** Overall layout of the test.

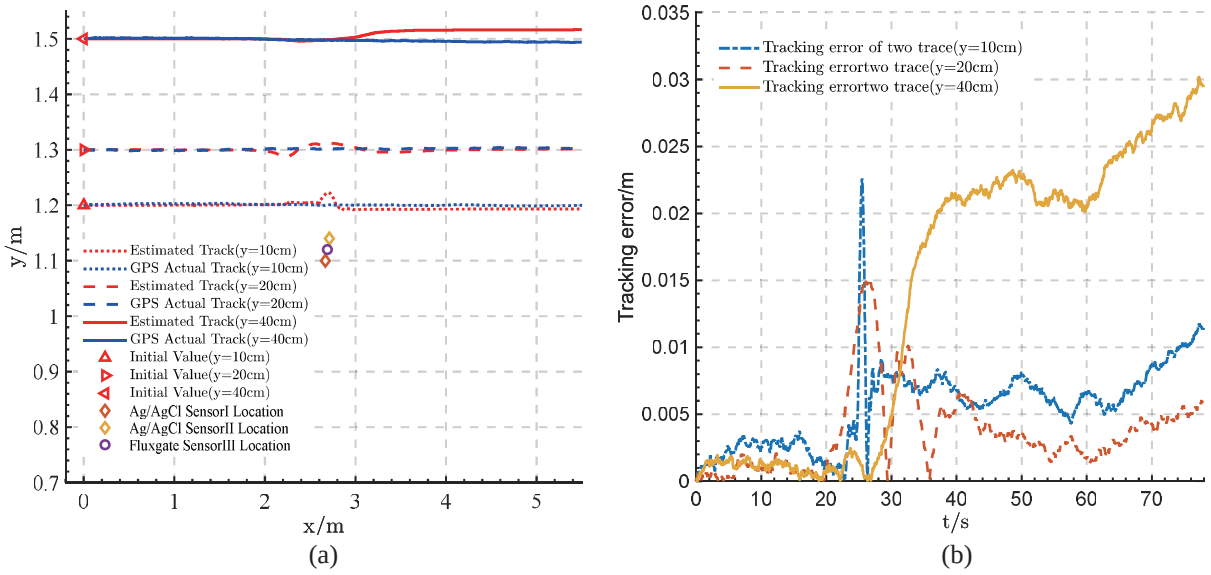


**Figure 6.** When the measured depth is 20 cm, the tracking calculation result of electromagnetic signals of different positive transverse distance. (a) The target tracking process diagram. (b) The tracking error result graph.

**Table 5.** Tracking results of different models in different water depths at different transverse distances.

| | | | | |
|---|---|---|---|---|
| **Tracking error less than 0.05 m** | **The positive horizontal distance is 10 cm** | | | |
| | Depth (cm) | Single electrical signal $S^{U}_{effect}$ (m) | Single magnetic signal $S^{B}_{effect}$ (m) | Joint electromagnetic signal $S^{UB}_{effect}$ (m) |
| | 20 cm | $4.9L$ | $5.1L$ | $5.5L$ |
| | 60 cm | $4.7L$ | $4.5L$ | $5.5L$ |
| | 100 cm | $3.6L$ | $3.7L$ | $4.7L$ |
| | **The positive horizontal distance is 20 cm** | | | |
| | Depth (cm) | Single electrical signal $S^{U}_{effect}$ (m) | Single magnetic signal $S^{B}_{effect}$ (m) | Joint electromagnetic signal $S^{UB}_{effect}$ (m) |
| | 20 cm | $4.7L$ | $4.7L$ | $5.5L$ |
| | 60 cm | $4.4L$ | $4.2L$ | $4.8L$ |
| | 100 cm | $3.5L$ | $3.6L$ | $4.4L$ |
| | **The positive horizontal distance is 40 cm** | | | |
| | Depth (cm) | Single electrical signal $S^{U}_{effect}$ (m) | Single magnetic signal $S^{B}_{effect}$ (m) | Joint electromagnetic signal $S^{UB}_{effect}$ (m) |
| | 20 cm | $4.4L$ | $4.1L$ | $5.5L$ |
| | 60 cm | $4.0L$ | $3.8L$ | $4.5L$ |
| | 100 cm | $3.7L$ | $3.6L$ | $4.0L$ |

## 5. JOINT ELECTROMAGNETIC SIGNAL TRACKING EXPERIMENT WITH SHIP MODEL

Based on the analog source experiments, the tracking model is further validated using a scaled-down ship model with the same sensor arrangement as the equivalent source experiments, and the ship model arrangement is shown in Figure 7.

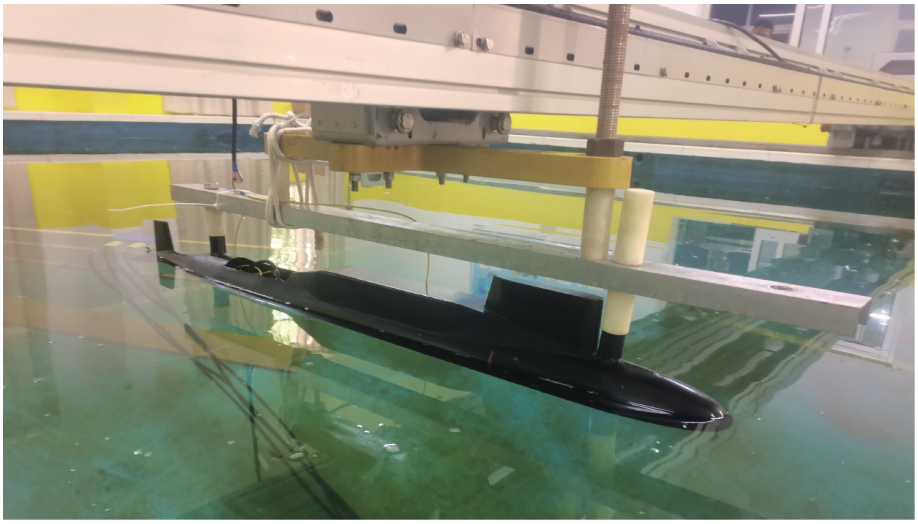

**Figure 7.** Submarine model layout.

**Table 6.** Tracking results of different models in different water depths at different transverse distances.

| | | | | |
|---|---|---|---|---|
| **Tracking error less than 0.05 m** | **The positive horizontal distance is 10 cm** | | | |
| | Depth (cm) | Single electrical signal $S^{U}_{effect}$ (m) | Single magnetic signal $S^{B}_{effect}$ (m) | Joint electromagnetic signal $S^{UB}_{effect}$ (m) |
| | 20 cm | $4.9L$ | $5.1L$ | $5.5L$ |
| | 60 cm | $4.7L$ | $4.5L$ | $5.5L$ |
| | 100 cm | $3.6L$ | $3.7L$ | $4.7L$ |
| | **The positive horizontal distance is 20 cm** | | | |
| | Depth (cm) | Single electrical signal $S^{U}_{effect}$(m) | Single magnetic signal $S^{B}_{effect}$ (m) | Joint electromagnetic signal $S^{UB}_{effect}$ (m) |
| | 20 cm | $4.7L$ | $4.7L$ | $5.5L$ |
| | 60 cm | $4.4L$ | $4.2L$ | $4.8L$ |
| | 100 cm | $3.5L$ | $3.6L$ | $4.4L$ |
| | **The positive horizontal distance is 40 cm** | | | |
| | Depth (cm) | Single electrical signal $S^{U}_{effect}$ (m) | Single magnetic signal $S^{B}_{effect}$ (m) | Joint electromagnetic signal $S^{UB}_{effect}$ (m) |
| | 20 cm | $4.4L$ | $4.1L$ | $5.5L$ |
| | 60 cm | $4.0L$ | $3.8L$ | $4.5L$ |
| | 100 cm | $3.7L$ | $3.6L$ | $4.0L$ |

The submarine ship model is 1.5 m long. The experimental parameters are set the same as in Table 4. An electrode is arranged in the boat to form a current loop with the propeller at the stern. The electrode distance is set to 80 cm, and the electrode input current is 225 mA.

When the measured water depth is 20 cm, the tracking results for the positive transverse distance of the target are 10 cm, 20 cm, and 40 cm, respectively, shown in Figure 8.

Varying the measured water depth and tracking the motion process of targets with different positive transverse distances at different depths, the tracking results of the joint electromagnetic signal are shown in Table 6.

In order to further verify the tracking effect of the combined electromagnetic signals, Gaussian

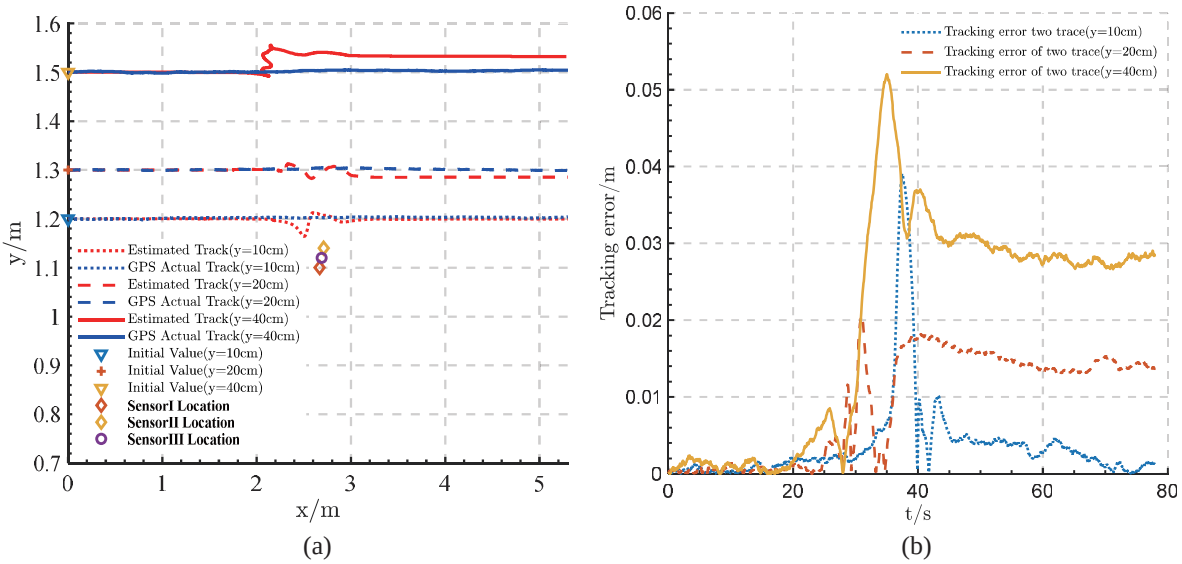


**Figure 8.** When the measured depth is 30 cm, the tracking calculation result of electromagnetic signals of different positive transverse distance. (a) The target tracking process diagram. (b) The tracking error result graph.

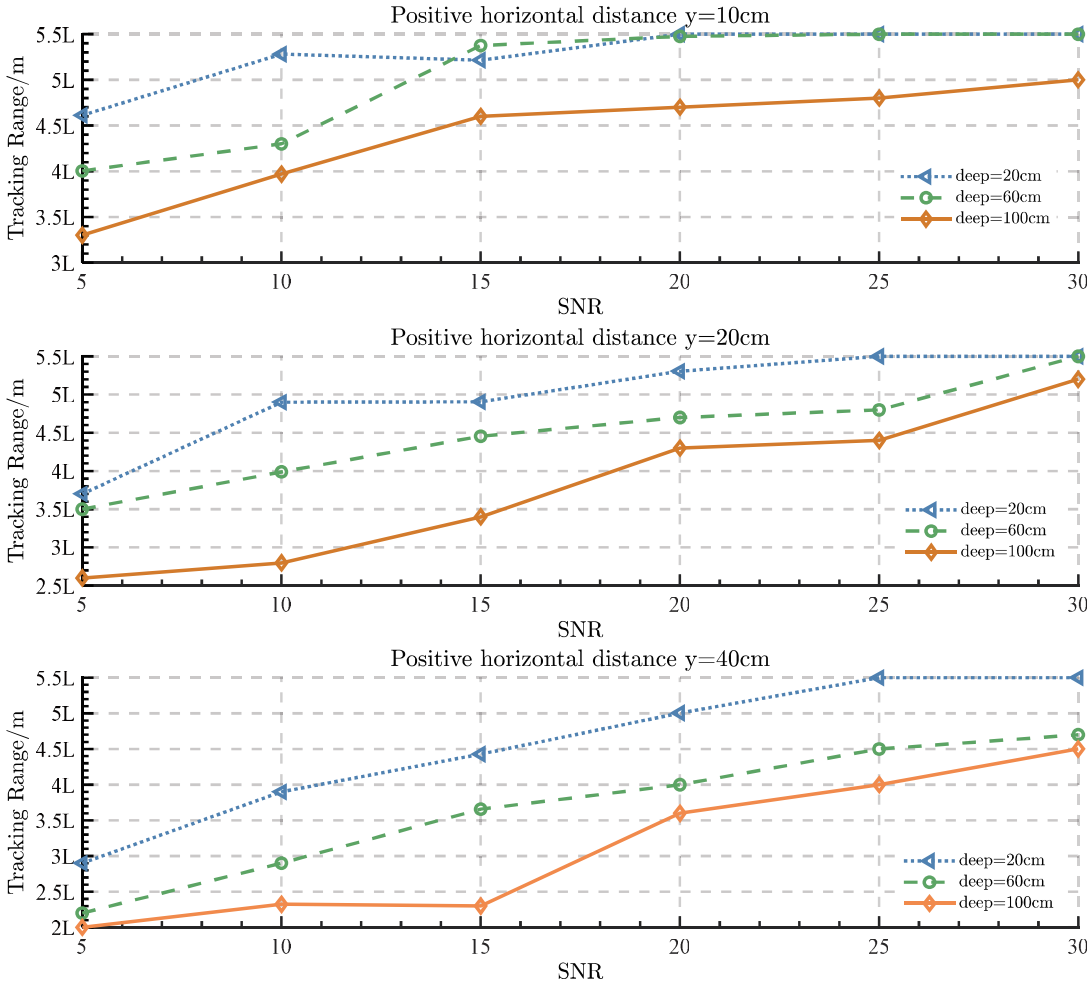


**Figure 9.** Tracking effect of different SNR, different positive horizontal distance and different depth.

white noise with signal-to-noise ratios of 5, 10, 15, 20, 25, and 30 was added to the collected signals, and the tracking distances at different positive transverse distances and different depths were calculated as shown in Figure 9.

As shown in Figure 9, when different signal-to-noise ratios are added to the acquired signals, the tracking range decreases with the increase of the measurement depth and improves with the increase of the signal-to-noise ratio when the positive transverse distance is the same as follows.

(1) When the signal-to-noise ratio is 20, a tracking range of $5.5L$ can be achieved at a measurement depth of less than 60 cm.

(2) When the positive transverse distance increases, the tracking effect becomes worse at the same S/N ratio, and only a tracking distance of $5.5L$ can be achieved at a S/N ratio of 25 when the measurement depth is 20 cm.

(3) The electromagnetic joint tracking method can achieve at least 2 times the tracking distance of the captain when the signal-to-noise ratio is only 5.

## 6. CONCLUSIONS

In order to realize the tracking of the target when the sensor carrying platform is a small-scale platform, this paper firstly proposes a target tracking model based on the theory of point charge and point magnetic charge for the joint electromagnetic signal, introduces the asymptotic update extended Kalman filter algorithm to simulate and verify the tracking method, and finally completes the simulated source experiment and ship model experiment in the laboratory. The main conclusions obtained are as follows.

(1) The proposed tracking model with joint electromagnetic signals in this paper can achieve the tracking of targets based on small-scale platforms.

(2) The simulation results show that the tracking error is less than 5 m in the range of 6 times the ship's length using the joint EM signal tracking method.

(3) Model experimental results show that the tracking error of 5.5 times the ship's length at a water depth of 20 cm is less than 0.05 m, and the tracking error of more than 2 times the ship's length can still be achieved when the signal-to-noise ratio is low, which proves the effectiveness of the tracking method.

The next step in the work is to conduct tests on a live ship at sea.

## REFERENCES

1. Cheng, J. F. and S. G. Gong, "Analysis of firing criteria of electric field fuse," *Journal of Naval University of Engineering*, Vol. 15, No. 4, 2003.
2. Luo, Y., Q.-M. Li, and H.-Y. He, "Study on electric field detection of ship based on character of gradient," *International Conference on Consumer Electronics*, IEEE, Jiangxi, China, 2011.
3. Wu, C. Q. and S. Zhao, "Study on the localization of the electric dipole sources," *Acta Physica Sinica*, Vol. 56, No. 9, 5180–5184, 2007.
4. Zhao, S. and C. Wu, "Matrix analysis of poly-dipole source localization," *Journal of Beijing Jiaotong University*, Vol. 32, No. 3, 56–59, 2008.
5. Bao, Z. H., S. G. Gong, J. Y. Sun, et al., "Localization of a horizontal electric dipole source embedded in deep sea by using two vector-sensors," *Journal of Naval University of Engineering*, Vol. 23, No. 3, 2011.
6. Wang, X., "Target localization based on two particular electric-field planes," *Chinese Journal of Ship Research*, Vol. 9, No. 4, 104–108, 2014.
7. Yu, P., J. Cheng, and J. Zhang, "Ship target tracking using underwater electric field," *Progress In Electromagnetics Research M*, Vol. 86, 49–57, 2019.
8. Donati, R. and J. P. Le Cadre, "Detection of oceanic electric fields based on the generalized likelihood ratio test (GLRT)," *IEEE Proceedings — Radar, Sonar and Navigation*, Vol. 149, No. 5, 221–230, 2002.
9. Zhang, J. W., R. X. Jiang, D. W. Xiao, et al., "Ship tracking based on the difference of electric potential," *Journal of Harbin Engineering University*, Vol. 41, No. 06, 812–816+831, 2020.

10. Wynn, W. M., C. P. Frahm, P. J. Carroll, et al., "Advanced superconducting gradiometer/Magnetometer arrays and a novel signal processing technique," *IEEE Transactions on Magnetics*, Vol. 11, No. 2, 701–707, 1975.
11. Wynn, W. M., "Magnetic dipole localization using the gradient rate tensor measured by a five-axis magnetic gradiometer with known velocity," *Proceedings of SPIE — The International Society for Optical Engineering*, Vol. 2496, 357–367, 1995.
12. Wahlström, N., J. Callmer, and F. Gustafsson, "Magnetometers for tracking metallic targets," *Information Fusion Conference*, IEEE, New York, 2011.
13. Birsan, M., "Electromagnetic source localization in shallow waters using Bayesian matched-field inversion," *Inverse Problems*, Vol. 22, No. 1, 43, 2005.
14. Wilson, M. A., S. A. Mccarthy, P. J. Collin, et al., "Alkene transformations catalysed by mineral matter during oil shale pyrolysis," *Organic Geochemistry*, Vol. 9, No. 5, 245–253, 1986.
15. Emerson, D. W., D. A. Clark, and S. J. Saul, "Magnetic exploration models incorporating remanence, demagnetization and anisotropy: HP 41C handheld computer algorithms," *Exploration Geophysics*, Vol. 16, No. 1, 1–122, 1985.
16. Wang, J. G., C. S. Lin, and S. G. Gong, "Algorithm of locating magnetic objects based on neural networks," *Journal of the Naval Academy of Engineering*, 2000.
17. Wang, J. G. and S. G. Gong, "Research on the problem of localizing magnetic target based on motion scalar magnetometer," *Acta Electronica Sinica*, Vol. 30, No. 7, 1057–1060, 2002.
18. Wu, Y. and Y. Sun, "Magnetic dipole target tracking based on recursive update Kalman filter," *Journal of Bjing University of Aeronautics and Astronautics*, Vol. 43, No. 9, 1805–1812, 2017.
19. Shan, S., S. H. Zhou, Z. H. Dai, and H. X. Zhang, "Strong tracking progressive update extended Kalman filter and its application in magnetic dipole tracking," *Journal of Naval University of Engineering*, Vol. 34, No. 01, 105–112, 202.
20. Wang, K. R., Y. D. Zhang, and Y. H. Liu, "Research on target organ motion tracking method based on the fusion of inertial navigation and electromagnetic navigation," *Journal of Instruments and Meters*, Vol. 9, No. 11, 177–187, 2020.
21. Guo, J. Q. and Y. P. Zhao, "A method of electromagnetic parameter selection for ray-tracing channel simulation," *Journal of Radio Wave Science*, Vol. 37, No. 01, 99–105, 2022.
22. Xing, K., "Application of tracking detection with transient electromagnetic method in driving roadways," *Shanxi Coal*, 2017.
23. Guo, C. B. and Q. Q. Yin, "Magnetic monopole array model for modeling ship magnetic signatures," *Acta Physica Sinica*, Vol. 68, No. 11, 114101, 2019.
24. Zanetti, R., "Adaptable recursive update filter," *Journal of Guidance, Control, & Dynamics*, Vol. 38, No. 7, 1295–1300, 2015
25. Huang, Y. L., Y. G. Zhang, N. Li, et al., "Gaussian approximate filter with progressive measurement update," *Proceedings of the 54th Annual Conference on Decision and Control*, 4344–4349, IEEE, Osaka, Japan, 2015
26. Zhang, J. W., P. Yu, R. X. Jiang, and B. Q. Sun, "Research on target tracking method based on ship electric field," *Journal of Military Engineering*, Vol. 41, No. 03, 559–566, 2020.
27. Jiang, R. X., X. G. Chen, and J. W. Zhang, *Ship Electric Fields and Their Applications*, Defense Industry Press, 2021.
28. Liu, J. S. and S. J. Rong, "Calculation of magnetic charges in equivalent transformation between molecular current and magnetic dipole," *Journal of Liaoning Normal University (Natural Science Edition)*, 2003.
29. Yu, P., J. W. Zhang, J. F. Cheng, et al., "Analysis of the natural electric field at different sea depths," *Journal of Instrumentation*, Vol. 16, No. 1, P01006–P01006, 2021.
30. Zhao, H., Y. G. Li, S. M. Duan, and Z. H. Xu, "Characterization of the response of seawater motion induced magnetic field to typhoon," *Journal of Ocean University of China (Natural Science Edition)*, 1–8, April 20, 2022.